Mobility was a Significant Determinant of Reported COVID-19 Incidence During the Omicron Surge in the Most Populous U.S. Counties

Jeffrey E. Harris MD PhD*† March 16, 2022

Abstract: We studied the relationship between declines in mobility and subsequently reported COVID-19 case incidence in 111 of the most populous U.S. counties during the Omicron surge from December 2021 through February 2022. We employed principal component analysis to construct a one-dimensional summary measure of the six Google mobility categories that are regularly reported for each county. Among counties with a lower mobility decline between December 20 and January 3, reported COVID-19 incidence did not peak until the week ending January 17, whereas among counties with a higher mobility decline, incidence peaked earlier by the week ending January 10 and remained significantly lower. Based upon a fixed-effects, longitudinal cohort model, we estimated that every 1-percent decline in mobility between December 20 and January 3 was associated with a 0.63 percent decline in peak incidence during the week ending January 17 (95% confidence interval, 0.40-0.86 percent). Based upon a cross-sectional analysis including mean household size and vaccination participation as covariates, we estimated that the same 1-percent decline in mobility was associated with a 0.36 percent decline in cumulative reported COVID-19 incidence from January 10 through February 28 (95% CI, 0.18-0.54 percent). Omicron did not simply sweep through the U.S. population until it ran out of susceptible individuals to infect. To the contrary, a significant fraction managed to avoid infection by engaging in risk-mitigating behaviors. More broadly, the behavioral response to perceived risk should be viewed as an intrinsic component of the natural course of epidemics in humans.

* Professor of Economics, Emeritus, Massachusetts Institute of Technology, Cambridge MA 02139; Physician, Eisner Health, Los Angeles CA 90015. Email: *jeffrey@mit.edu*

† This study relies exclusively on publicly available data that contain no individual identifiers. The author has no competing interests and no funding sources to declare. This article represents the sole opinion of its author and does not necessarily represent the opinions of the Massachusetts Institute of Technology, Eisner Health, or any other organization. Supporting programs and data have been posted at https://osf.io/6edyc/.

Introduction

During the early and middle phases of the COVID-19 pandemic, numerous studies in various countries documented an association between a decline in population mobility and a subsequent reduction in reported case incidence [1-9]. The principal objective of the present study is to begin to assess whether this mobility-incidence relationship similarly prevailed during the more recent wave driven by the Omicron variant of SARS-CoV-2.

There are several critical reasons why the mobility-incidence relationship observed for the ancestral strain and prior variants of SARS-CoV-2 may not apply equally to Omicron. More than any other variant, Omicron exhibited significant immune escape against vaccination and prior infection [10, 11], though vaccines continued to protect against serious disease [12, 13]. Omicron appears to have been about twice as transmissible as the Delta variant [14], with the larger proportion of asymptomatic Omicron infections likely enhancing the prevalence of super spreaders [15]. While home testing rose markedly in response to the initial news of the variant [16], later reports of Omicron's tendency to spare the deep tissues of the lung [17] may have alleviated fears of serious illness that drive voluntary risk-mitigation behavior [18]. There is the further concern that frequently changing news reports and public health guidance induced "worry fatigue" [19], especially when perceptions of risk and compliance with such guidance are themselves subject to herd transmission [20].

Mobility is a multidimensional concept that has been variously gauged by such diverse measures as smartphone visits to bars and restaurants [21], traffic patterns [9], and television watching as a proxy for time spent at home [22]. Here, following the lead of two key papers [23, 24], we employ the statistical technique of principal component analysis to collapse the six-dimensional Google Mobility Reports [25] into a single mobility indicator. Further adhering to a recent study of reported case incidence and hospitalization in relation to vaccination rates during the Delta surge [26], we restrict our analysis to the most populous counties in the United States, together comprising approximately 44 percent of the total U.S. population. Such an approach avoids the potential pitfalls of comparing small rural counties with large urban centers. We focus on the wave of reported cases from December 2021 through Feb 2022, during which Omicron was far and away the dominant variant [27].

Data

Most Populous Counties

As noted above, we confined our analysis to the most populous counties in the United States. From an *initial sample* of all 112 counties with population exceeding 600,000, we excluded one county (Johnson County KS, population 602,000) as a result of missing data on one of the mobility measures to be described below. Our *analytic sample* thus consisted of 111 counties, together comprising 146.5 million persons or about 44 percent of the entire U.S. population. Appendix Fig. A maps the locations of all 112 counties in the initial sample, identifying the excluded county as well.

Google Mobility Reports

We relied upon Google Mobility Reports [25] to assess changes in mobility in each of the 111 counties in our analytic sample. Compiled from data on the movements of mobile devices, these reports provided daily measures of mobility for six distinct categories of places: retail & recreation; grocery & pharmacy; parks; transit stations; workplaces; and residential [28]. Based upon the number of visits to and length of stay in the places in each category, the reports showed activity as a percent of baseline, where the baseline represented the median value for the corresponding day of the week during the 5-week period from January 3 – February 6, 2020. For each of the 111 counties in the analytic sample and each of the six categories of mobility, we computed weekly mean values of mobility for the week ending Monday, February 24, 2020, through the week ending Monday, February 28, 2022. We chose a weekly ending date of Monday solely to be conformal with the available data on COVID-19 case reports, to be described below.

Community Profile Reports

We relied upon the COVID-19 Community Profile Reports, issued regularly by the White House COVID-19 Team [29], for data on the reported number of COVID-19 cases in each county for each week, starting with the week ending December 6, 2021, and continuing through the week ending February 28, 2022. We also relied upon this data source for estimates of each county's population, from which we computed COVID-19 incidence rates, as well as two county-specific demographic characteristics: the U.S. Center for Disease Control's social vulnerability index [30], and the average household size. We included the latter characteristic to capture the important influence of intra-household transmission on COVID-19 incidence [3].

County-Specific Vaccination Data

In addition to the foregoing county-specific demographic variables, we relied upon a database of COVID-19 vaccination participation rates, compiled by the U.S. Centers for Disease Control and Prevention [31]. These data showed the percentage of each county's population who completed a one- or two-dose series of vaccinations, as well as the cumulative number of booster doses per 100 population, as of December 15, 2021, the earliest date for which both measures were available.

Statistical Methods

Principal Component Analysis of Google Mobility Categories

We relied upon the data on the six weekly Google mobility measures in the 111-county database, covering the 106-week period from the week ending February 24, 2020, through the week ending February 28, 2022, to compute the first principal component as a summary measure of mobility [23, 24]. This summary measure, which we refer to here as our *mobility indicator*, represents the linear combination of the six individual mobility categories that captures the largest fraction of the overall variance of the data [32]. Denoting by g_{kit} the observed value of Google mobility category k in county i during week t, we thus computed the indicators $x_{it} = \sum_{k=1}^{6} \zeta_k g_{kit}$, where the estimated coefficients ζ_k were not necessarily positive, but where $\sum_{k=1}^{6} \zeta_k^2 = 1$. For this and other statistical computations, we relied upon Stata 17 software [33].

County-Specific Changes in Mobility

Having relied upon the entire database of multidimensional Google mobility categories from the week ending February 24, 2020, onward to compute our unidimensional mobility indicator, we then focused on the narrower 13-week period from the week ending December 6, 2021 through the week ending February 28, 2022, which encompassed the Omicron surge in the United States [27].

As described in detail in the Results below, we determined that our mobility indicator x_{it} (where i = 1, ... ,111 and t = 1, … ,13) declined primarily during the interval between the week ending December 20, 2021 (that is, t = 3) to the week ending January 3, 2022 (that is, t = 5). For each county i, we thus computed the change in the mobility indicator $\Delta x_i = x_{i5} - x_{i3}$. Since mobility declined overall during the 13-week analysis period, the quantities Δx_i were negative. We then divided the sample of counties into the lower half and upper half of the distribution of

the absolute values $|\Delta x_i|$, denoting counties in the lower half as *low mobility decline* and those in the upper half as *high mobility decline*. We defined the binary variable X_i to equal 0 if county i was in the lower half and 1 if county i was in the upper half of the distribution.

Longitudinal Cohort of Counties

The available data, described above, thus allowed us to construct a longitudinal cohort of 111 counties, indexed i = 1, …, 111, covering the 13-week period running from the week ending December 6, 2021 (t = 1) through the week ending February 28, 2022 (t = 13). For each county i and week t, we had data not only on our constructed mobility indicator x_{it}, but also on y_{it}, the incidence of reported cases of COVID-19 per 100,000 population.

To examine the qualitative relationships between changes in mobility and changes in COVID-19 incidence, we first plotted the population-weighted mean values of x_{it} and y_{it} over time for the two groups of counties with low and high declines in mobility. For example, the population-weighted mean mobility indicator among low-decline counties at week t would equal $\sum_{X_i=0} r_i x_{it} / \sum_{X_i=0} r_i$, where r_i is the population of county i and where the summations are only over those counties i for which X_i = 0. The other conditional means were computed analogously.

To further examine the quantitative relationships between changes in mobility and changes in COVID-19 incidence, we estimated a fixed-effects longitudinal cohort model with the following specification:

$$y_{it} = \mu + \alpha_i + \gamma_t + \beta_t \Delta x_i + \varepsilon_{it} \qquad (1).$$

In equation (1), the parameter μ was an overall mean, while α_i and γ_t were county-specific and time-specific fixed effects, respectively. The parameters of interest β_t gauged the impact of county-specific changes in mobility on a week-by-week basis. Finally, ε_{it} were assumed to be spherical error terms. This fixed-effects model was estimated by ordinary least squares.

Cross-Sectional Analyses

To further study the quantitative relationships between changes in mobility and changes in COVID-19 incidence, we defined the cumulative incidence for each county i during the period from week ending January 10, 2022 (t = 6) through the week ending February 28, 2022 (t = 13) as $Y_i = \sum_{t=6}^{13} y_{it}$. We then ran the cross-sectional model:

$$\log Y_i = \eta + \theta\, \Delta x_i + \sum_j \lambda_j Z_{ij} + \nu_i \qquad (2).$$

In equation (2), the parameter η was an overall mean, while the parameters λ_j captured the effects of county-specific covariates Z_{ij}. The parameter of interest θ gauged the proportional impact the change in mobility during the period between December 20, 2021, and January 3, 2022, on the subsequent cumulative reported incidence of COVID-19 from the week ending January 10, 2022, onward. Finally, ν_i were assumed to be uncorrelated error terms. This cross-sectional model was estimated by population-weighted least squares.

Results

Mobility Indicator

Appendix Table A displays the estimated coefficients of the first principal component of the six Google mobility categories. The Google Retail & Recreation category of mobility had the largest contribution to the overall variance of our computed mobility indicator, while the Parks ctegory had the smallest contribution. The Residential category had a negative estimated coefficient, inasmuch as increases in visits to and duration of stay in residences reflected a decrease in overall mobility. To a first-order approximation, our estimated mobility indicator x was equal to $0.44 \times [\textit{Retail \& Recreation} + \textit{Grocery \& Pharmacy} + \textit{Transit Stations} + \textit{Workplaces} - \textit{Residences} + \frac{1}{2} \times \textit{Parks}]$.

Fig. 1 illustratively graphs the six Google mobility categories specifically for Philadelphia County, Pennsylvania (population 1,584,000), during the period from the week ending December 6, 2021 (t = 1), through the week ending January 31, 2022 (t = 9). Each of the colored piecewise linear plots shows the evolution of one of the original Google mobility categories g_{kit}. The thicker black plot shows the corresponding evolution of our unidimensional mobility indicator x_{it}, calculated from the coefficients in Appendix Table A. The path of this overall mobility indicator shows a significant decline during the two-week interval between the week ending December 20, 2021 (t = 3) and the week ending January 3, 2022 (t = 5).

Among the 111 counties under study, we observed a median absolute decline of 31.85 units in our calculated mobility indicator during the two-week interval between the week ending December 20, 2021 (t = 3) and the week ending January 3, 2022 (t = 5). Thus, we classified counties into the low-decline group (X_i = 0) if their observed absolute mobility decline was less

than this median value and into the high-decline group (X_i = 1) if their absolute mobility decline was greater than this median value.

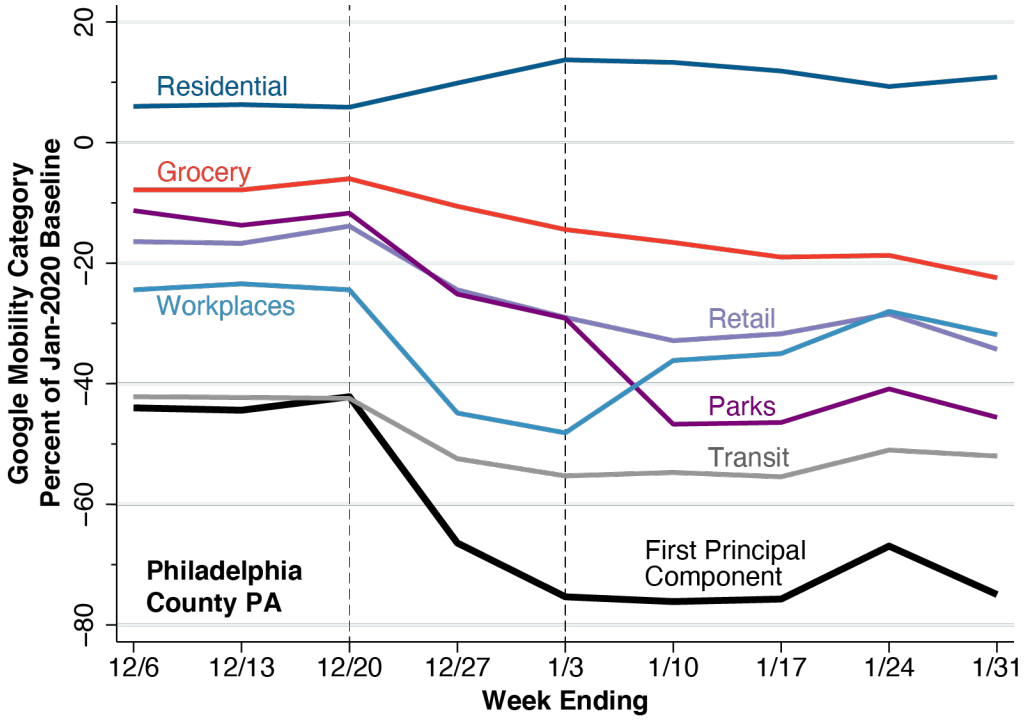

Fig. 1. Construction of Mobility Indicator as First Principal Component of Six Google Mobility Categories, Philadelphia County, Pennsylvania, Weeks Ending December 6, 2021, Through January 31, 2022. Each colored piecewise linear plot shows the evolution of the weekly mean of one of the six Google mobility categories. The thicker, black piecewise linear plot shows the first principal component of the six mobility categories as calculated for Philadelphia County. The drop in the calculated mobility indicator occurred during the two-week interval from week ending 12/20/21 to the week ending 1/3/22.

Fig. 2 displays illustrative paths of our unidimensional mobility indicator for 14 randomly selected counties in low-decline group (X_i = 0, left panel) and another 14 randomly selected counties in the high-decline group (X_i = 1, right panel). In both panels, we have highlighted the portions of each path covering the 2-week interval from December 10, 2021 – January 3, 2022. For the low-decline (X_i = 0) counties on the left, nearly all the calculated decline in overall mobility occurred during the first week. For the high-decline (X_i = 1) counties on the right, the calculated mobility indicators continued to decline during the second week.

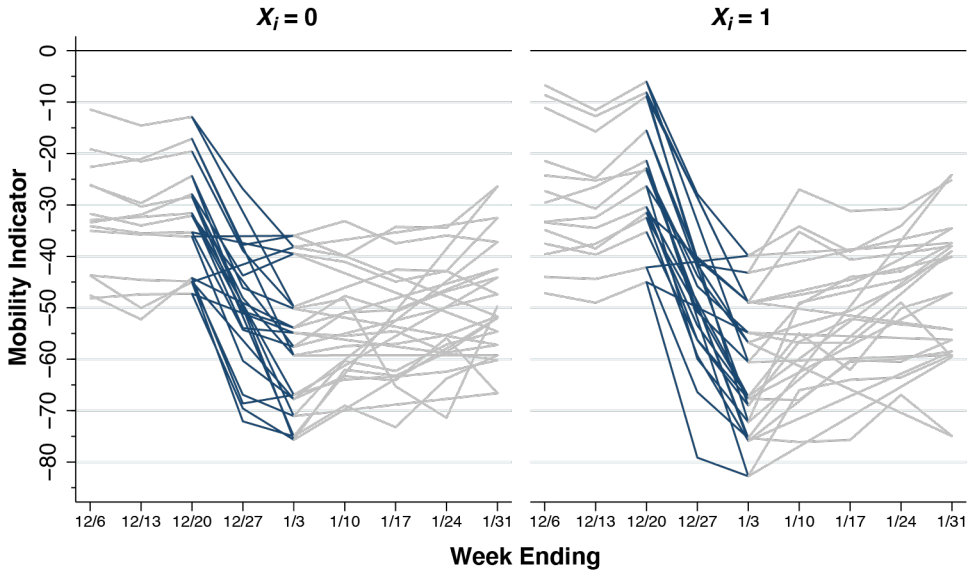

Fig. 2. Illustrative Paths of Mobility indicator in Counties with Low and High Declines During the Two-Week Interval Between December 20, 2021, and January 3, 2022. The panel on the left, identified as X_i = 0, shows the paths of 14 randomly selected counties with an absolute decline of less than 31.85. The panel of the right, identified as X_i = 1, shows the paths of another 14 randomly selected counties with an absolute decline more than 31.85. In both panels, the paths of the calculated mobility indicators during the interval from 12/20/21 – 1/3/22 have been highlighted. For the low-decline (X_i = 0) counties on the left, nearly all the calculated decline in mobility occurred during the first week, that is, during 12/20 – 12/27/21. For the high-decline (X_i = 1) counties on the right, the calculated mobility indicators continued to decline during the second week, that is, during 12/27/21 – 1/3/22.

Mobility and Case Incidence

Fig. 3 illustratively displays the combined paths of the mobility indicator x_{it} and the case incidence y_{it} specifically for Philadelphia County, Pennsylvania. The black-colored plot with square datapoints shows the path of the mobility indicator, replotted from the first principal component shown in Fig. 1, with the measurement scale along the left axis. The red-colored plot with circular datapoints, with measurement scale along the right axis, shows the path of COVID-19 case incidence in weekly reported cases per 100,000 population.

For Philadelphia County PA, our computed mobility indicator x_{it} declined from –42.15 during the week ending December 20, 2021, to –75.33 during the week ending January 3, 2022. The observed absolute decline of $|\Delta x_i|$ = 33.18 thus placed Philadelphia County in the high-decline (X_i = 1) group. One week later, by the week ending January 10, 2022, reported COVID-19 incidence reached a peak of 1,666 cases per 100,000 population and declined thereafter.

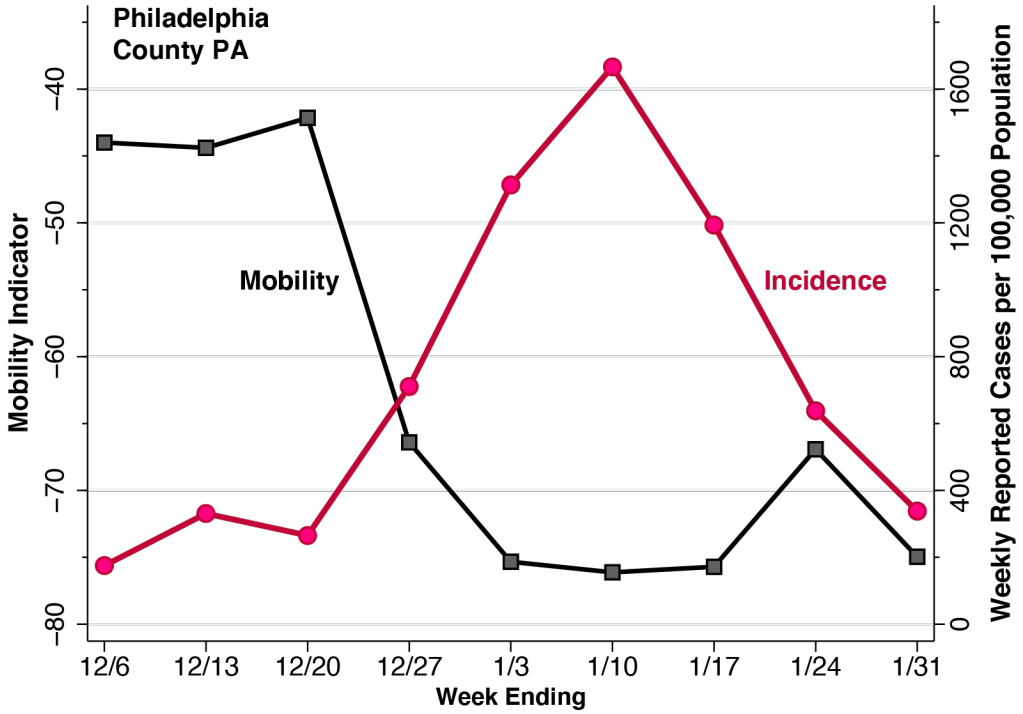

Fig. 3. Mobility Indicator (Left Axis) and Reported COVID-19 Cases (Right Axis) in Philadelphia County, Pennsylvania, During the Weeks Ending December 6, 2021, Through January 31, 2022. The black plot with square datapoints corresponds to the weekly mobility indicator calculated in Fig. 1. The red plot with circular datapoints corresponds to the weekly counts of reported cases of COVID-19 per 100,000 population. Mobility declined during the interval from the week ending 12/20/21 through the week ending 1/3/22. The rise in reported cases peaked during the week ending 1/10/22 and declined thereafter.

Longitudinal Cohort Analysis

For the low- and high-decline groups separately, Fig. 4 graphs the temporal paths of the population-weighted mean mobility indicator and population-weighted mean COVID-19 incidence during the 13-week study period. Both mobility and incidence have been computed as the change from the week ending December 6, 2021. Changes in mobility (square datapoints, measured on the left axis) are identified by the labels "Δ Mobility," while changes in incidence (circular datapoints, measured on the right axis) are identified by the labels "Δ Incidence."

Both the low- and high-decline counties followed essentially the same mobility path through the week ending December 27, 2021. During the subsequent week ending January 3, 2022, however, the two groups diverged, with the high-decline (X_i = 1) group exhibiting a greater continuing drop in mobility. These differences in mobility are reflected in the divergent paths of incremental COVID-19 incidence. Among low-decline (X_i = 0) counties, incidence

peaked during the week ending January 17, while among high-decline (X_i = 1) counties, incidence reached a lower peak one week earlier.

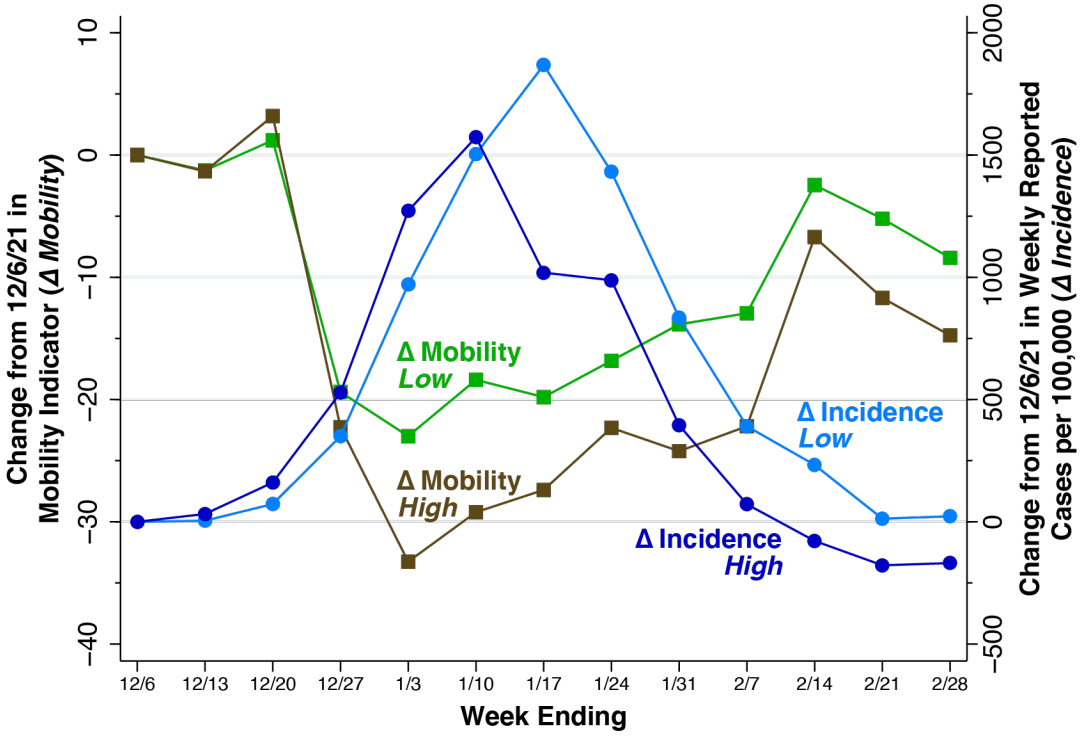

Fig. 4. Changes in Mobility Indicators (Δ *Mobility*, Left Axis) and Changes in Reported COVID-19 Cases (Δ *Incidence*, Right Axis) in Low and High Mobility Decline Counties, Weeks Ending December 6, 2021 Through February 28, 2022. Low mobility decline counties are identified as *Low*, while high mobility decline counties are identified as *High*. For both mobility and incidence, the figure plots the change from the week ending 12/6/21. Among low-decline (*Low*) counties, incremental incidence peaked during the week ending 1/17/22. Among high-decline (*High*) counties, incremental incidence peaked earlier during the week of 1/10/22 and declined earlier.

Appendix Table B shows our estimates of the parameters of the fixed-effects model of equation (1). Fig. 5 below graphs the estimates of the key parameters of interest β_t for each week from t = 2, …, 13, as derived from that model. Since t = 1 (ending December 6, 2021) was the reference category, the parameter β_1 was necessarily constrained to equal 1. The estimates of β_t from the week ending January 17 (t = 7) through the week ending February 14 (t = 11) are all positive and significant at the 5-percent level. For the peak week ending January 17, 2022, the estimated parameter was β_7 = 37.7 with 95% confidence interval 23.9–51.4 ($p < 0.001$). That is, an additional one-point drop in our mobility indicator was associated with an incremental decline of 37.7 weekly reported cases of COVID-19 per 100,000 population.

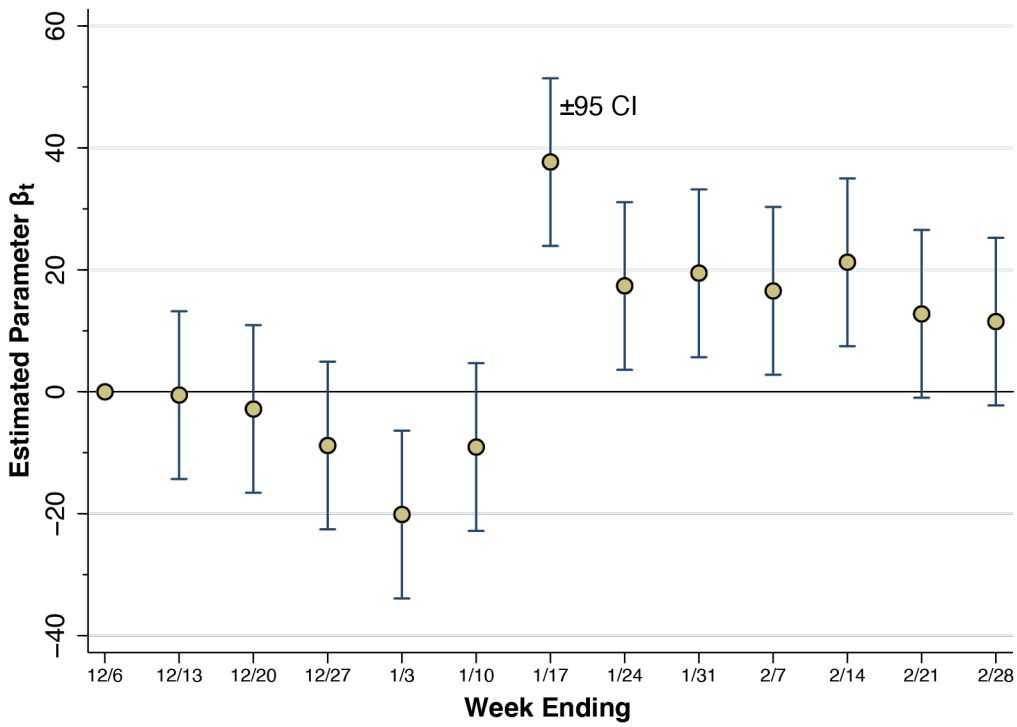

Fig. 5. Estimates of the Interaction Parameters β_t in the Longitudinal Model of Equation (1). Except for the reference week ending 12/6/21, each week t has its own interaction parameter β_t, which measures the marginal impact of a change in the mobility indicator from 12/20/21 to 1/3/22 (Δ *Mobility*) on the incremental reported incidence of COVID-19 cases per 100,000 population (Δ *Incidence*). The error bars surrounding each estimate are 95% confidence intervals. Starting with the week ending 1/17/22 and continuing through the week ending 2/14/22, the estimated parameters were positive and the null hypothesis of no association with changes in mobility could be rejected at the 5-percent level.

Based upon the observed sample means, we can reinterpret this estimated peak marginal effect β_7 as an elasticity. With a population-weighted mean reported incidence of 1,729 cases per 100,000 during the week ending January 17, each one-point drop in mobility is thus associated with a $37.7/1729$ = 2.18 percent drop in incidence (95% CI, 1.38–2.97 percent). At the population-weighted mean value of Δx equal to –29.04, each one-point decrease represents a $1/29.04$ = 3.44 percent decline in mobility. Thus, we obtain an estimated elasticity of $2.18/3.44$ = 0.63 with a 95% confidence interval of 0.40–0.86.

Cross-Sectional Results

Appendix Table C displays our estimates of the parameters of the cross-sectional model of equation (2). The estimated parameter θ was significantly different from zero in a bivariate specification on the change in mobility (specification A) as well as in multivariate specifications (B and C) that included demographic covariates and vaccination participation rates. Apart from

the change in mobility, average household size was the only other explanatory variable exhibiting a statistically significant association with cumulative reported COVID-19 incidence.

Fig. 6 plots the cumulative cases per 100 population between the week ending January 10, 2022, and the week ending February 28, 2022 (that is, the variable Y_i in equation (2)) against the change in our calculated mobility indicator (Δx_i) between December 20, 2021, and January 3, 2022 (that is, the variable Δx_i). In accordance with the log-linear specification of equation (2), the vertical axis is measured on a logarithmic scale. The size of each datapoint reflects the county population.

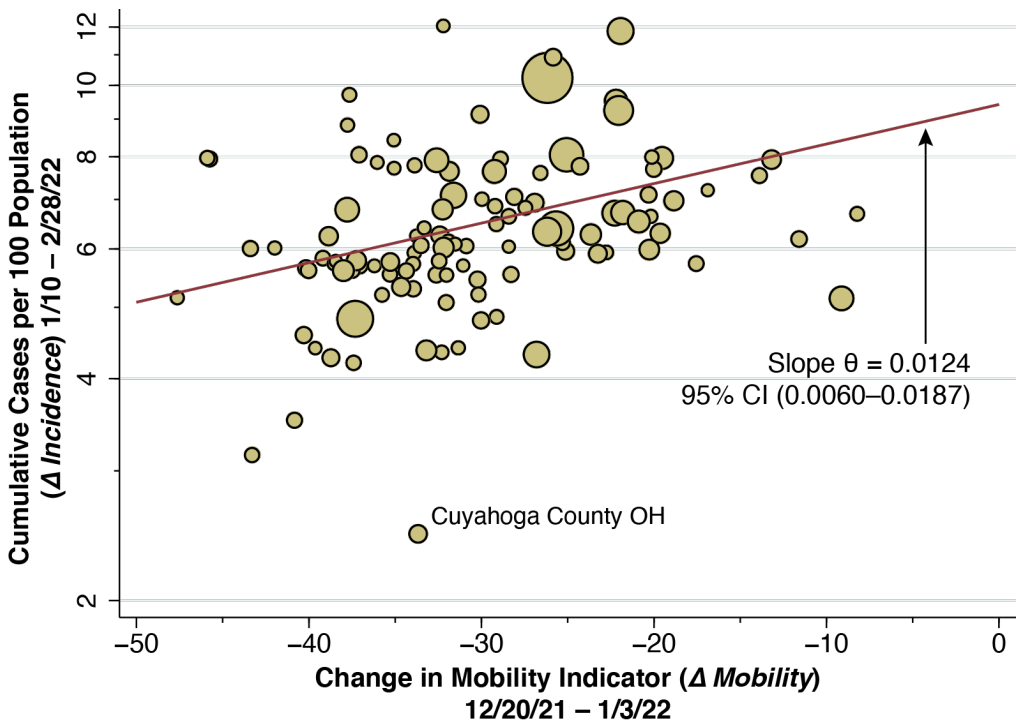

Fig. 6. Cumulative Reported COVID-19 Cases per 100 Population During January 10 Through February 28, 2022 (Δ *Incidence*) Versus the Change in the Mobility Indicator During December 20, 2021, Through January 3, 2022 (Δ *Mobility*), Plotted for 111 Counties. The size of each datapoint reflects the county population. Cumulative reported COVID-19 cases are plotted on a logarithmic scale. The weighted least squares fitted line is shown in red. The estimated slope, corresponding to the parameter θ in equation (2) was 0.0124 with 95% CI (0.0060, 0.0187). That is, every additional 1-point reduction in the mobility indicator was associated with a 1.24 percent decline in cumulative reported cases per 100 persons. The outlier in the plot is identified as Cuyahoga County, Ohio. The vertical axis plots cumulative case incidence from the week ending January 10 onward. Cumulative incidence for the entire Omicron wave, from the week ending December 6, 2021, averaged 9 per 100 population.

The superimposed line represents the population-weighted least squares fit to the data. This corresponds to the bivariate regression of $\log Y_i$ versus Δx_i without additional covariates Z_i, shown as specification A in Appendix Table C. The estimate of the slope parameter θ was

0.0124, with 95% confidence interval 0.0060–0.0.187. We can similarly reinterpret this cumulative marginal effect as an elasticity. Thus, every additional one-point decrease in our calculated mobility indicator was associated with a 1.24 percent decline in cumulative case incidence. At the population-weighted mean value of Δx equal to –29.04, each one-point decrease represents a $1/29.04$ = 3.44 percent decline in mobility. Thus, we obtain an estimated elasticity of $1.24/3.44$ = 0.36 with a 95% confidence interval of 0.18–0.54.

Discussion

Interpreting Elasticities

For each one-percent decline in our unidimensional measure of motility, which we derived from the six-dimensional Google Mobility categories, we have estimated a 0.63-percent decline in peak reported case incidence (95% confidence interval, 0.40 to 0.86 percent) and a 0.36-percent decline in cumulative reported case incidence (95% confidence interval, 0.18 to 0.54 percent). That the short-term elasticity of peak incidence turns out to be greater than the longer-term elasticity of cumulative incidence is hardly unexpected. As the prevalence of infection falls beyond the peak of epidemic wave, the effectiveness of risk-avoidance measures would be expected to decline. The declining marginal effects derived from the longitudinal cohort model, as seen in Fig. 5, are consistent with this interpretation.

Nor is it unexpected that the estimated mobility-incidence elasticity should be less than 1 even at the peak of the Omicron wave. For it implies that there were some sources of infection whose risks could not be mitigated through the available mobility-reduction strategies. Consider, for example, an individual whose only source of infection was taking public transport to work. If she cut back her exposure through this modality by x percent, her risk of infection would likewise decline by x percent, and the mobility-elasticity elasticity would be 1. If, on the other hand, intrahousehold transmission from family members was a second, independent source of infection, then her cutting back on public transport by x percent would lower her infection risk by less than x percent, and the corresponding elastic would be less than unity. Our finding that average household size was a significant determinant of county-specific Omicron case incidence (Appendix Table C) suggests that this example is more than hypothetical.

Changes in Behavior as an Intrinsic Feature of Course of Epidemics in Humans

Our results belie the hypothesis that Omicron simply swept through the population until the variant ran out of susceptible individuals to infect. For the entire Omicron surge, cumulative reported incidence averaged approximately 9 cases per 100 population (Fig. 6). If only one-fourth of all Omicron infections were reported by public authorities [34], then approximately 36 percent of the population became infected during the Omicron surge. In view of Omicron's documented capacity for immune escape from vaccination and prior infection [10, 11], there had to be no small fraction of susceptible individuals who, by engaging in risk-mitigating behaviors, managed to avoid infection.

Our findings reinforce the broader conclusion that the behavioral response to perceived risk needs to be regarded as an intrinsic component of the course of epidemics in humans. Quite apart from the evidence now accumulated in the ongoing COVID-19 pandemic, such behavioral responses have been documented for HIV in developing countries [35], the SARS outbreak in Hong Kong [36], the swine flu outbreak [37], the H1N1 influenza outbreak [38], and sexually transmitted diseases generally [39].

The Argument for Reverse Causation

The principal objection to our findings is that our study design cannot demonstrate a purely causal relation between initial declines in mobility and subsequent reductions in the incidence of infection. To the contrary, the argument goes, the observed declines in our unidimensional mobility indicator between the week ending December 10, 2021, and the week ending January 3, 2022, could also have been an early *response* to the emerging Omicron wave. One might conjecture, in fact, that the somewhat greater COVID-19 incidence in high-mobility-decline counties seen in Fig. 4, especially during the week ending January 3, was in fact the stimulus for the inhabitants of those counties to continue to engage in mobility-reducing behaviors. Such an interpretation would seem to square with the significant negative estimate of the parameter β_5 in Fig. 5.

In view of such reverse causation, our estimates of the parameters β_7 through β_{13} in Fig. 5, covering the period from the week ending January 13 onward, may indeed be biased upward, as is our cross-sectional slope parameter θ in Fig. 6. However, the magnitude of the bias is likely to be small. After all, the striking temporal relation between the extent of the mobility reductions

observed through the week ending January 3 and the *subsequent* divergence in COVID-19 incidence, as seen in Fig. 4, cannot readily be explained by reverse causation.

Policy Endogeneity

It would have been preferable, some might contend, to instead construct predictor variables based upon the extent of policy restrictions on mobility imposed in each county, such as renewed requirements on indoor mask use. In principle, such restrictions would be regarded as exogenous instruments to identify the unbiased effect of the endogenous mobility indicator that we have relied upon here [40]. The problem with this approach is that policies intended to restrict mobility are likewise endogenous. A public authority's decision to impose a mask mandate may just as well be a response to news of rising COVID-19 cases as an individual's uncoerced decision not to take the subway.

There is little basis to suppose, in any event, that declines in mobility such as those consistently observed in Figs. 1 through 4 are necessarily responses to coercive measures by public authorities. The near collapse of subway ridership in New York City during the second week of March 2020 was followed within 1–2 weeks by the flattening of the COVID-19 incidence curve. Yet no government authority ordered New Yorkers to stop taking the subway en masse [4].

Appropriateness of a Unidimensional Mobility Indicator

The data in Figs. 1 through 4 make a strong case in favor of the suitability of our unidimensional summary indicator of the six Google mobility categories. In the illustrative plot in Fig. 1, we saw how five of the individual categories tended to move together, while the residential category tended to move in the opposite direction. Our principal component analysis (Appendix Table A) confirmed these observations and further demonstrated that visits to retail establishments captured a larger fraction of the overall variance of the six categories. In the illustrative plot of Fig. 2, we saw how the resulting unidimensional indicator consistently captured changes in mobility during the two-week interval from the week ending December 20 to the week ending January 3. In Figs. 3 and 4, we saw how the temporal path of our unidimensional mobility indicator during that interval was followed by a peaking in reported Omicron cases one week later.

Cross-Sectional Analysis with Covariates

In our longitudinal cohort analysis of equation (1), we relied on the statistical technique of fixed effects to capture other, persistent unobserved characteristics of individual counties. In the cross-sectional analysis of equation (2), by contrast, we relied upon county-specific demographic variables and indicators of vaccination participation. Unfortunately, we did not have county-specific data on booster vaccinations before December 15, 2021. Consequently, our data may include a nontrivial number of recent vaccinations in response to emerging news about the coming Omicron wave.

In contrast to our longitudinal study of a cohort of 111 counties over 13 successive weeks, our cross-sectional analysis encompassed only 111 county-specific observations on cumulative reported COVID-19 incidence. As already noted, reported cases of Omicron may have constituted no more than one-quarter of all incident cases [34]. This observation raises the possibility that the degree of underreporting in a particular county was related to the magnitude of the observed decline in mobility. To the extent that counties with a higher perceived risk and greater self-imposed declines in mobility also reported more cases, our cross-sectional estimates would understate the strength of the mobility-incidence relationship.

Conclusion

Our results confirm a quantitative relationship between declines in mobility and subsequent declines in reported case incidence during the Omicron surge in the most populous counties in the United States. Our findings further imply that a significant fraction of the population managed to avoid infection by engaging in risk-mitigating behaviors. More broadly, the behavioral response to perceived risk should be viewed as an intrinsic component of the natural course of epidemics in humans.

References

1. Harris, J.E., *COVID-19, bar crowding, and the Wisconsin Supreme Court: A non-linear tale of two counties.* Research in International Business and Finance, 2020. **54**: p. 101310.
2. Harris, J.E., *Data from the COVID-19 epidemic in Florida suggest that younger cohorts have been transmitting their infections to less socially mobile older adults.* Review of Economics of the Household, 2020. **18**(ePub August 22): p. 1019-1037.
3. Harris, J.E., *Los Angeles County SARS-CoV-2 Epidemic: Critical Role of Multi-generational Intra-household Transmission.* Journal of Bioeconomics, 2021. **23**: p. 55-83.
4. Harris, J.E., *Critical Role of the Subways in the Initial Spread of SARS-CoV-2 in New York City.* Front Public Health, 2021. **9**: p. 754767.
5. Kephart, J.L., et al., *The effect of population mobility on COVID-19 incidence in 314 Latin American cities: a longitudinal ecological study with mobile phone location data.* Lancet Digit Health, 2021. **3**(11): p. e716-e722.
6. Oh, J., et al., *Mobility restrictions were associated with reductions in COVID-19 incidence early in the pandemic: evidence from a real-time evaluation in 34 countries.* Sci Rep, 2021. **11**(1): p. 13717.
7. Nouvellet, P., et al., *Reduction in mobility and COVID-19 transmission.* Nat Commun, 2021. **12**(1): p. 1090.
8. He, S., et al., *Delay in the Effect of Restricting Community Mobility on the Spread of COVID-19 During the First Wave in the United States.* Open Forum Infect Dis, 2022. **9**(1): p. ofab586.
9. Manzira, C.K., A. Charly, and B. Caulfield, *Assessing the impact of mobility on the incidence of COVID-19 in Dublin City.* Sustain Cities Soc, 2022. **80**: p. 103770.
10. Dejnirattisai, W., et al., *SARS-CoV-2 Omicron-B.1.1.529 leads to widespread escape from neutralizing antibody responses.* Cell, 2022. **185**(3): p. 467-484 e15.
11. Andrews, N., et al., *Covid-19 Vaccine Effectiveness against the Omicron (B.1.1.529) Variant.* N Engl J Med, 2022.
12. Liu, J., et al., *Vaccines elicit highly conserved cellular immunity to SARS-CoV-2 Omicron.* Nature, 2022.
13. U.S. National Institutes of Health, *COVID-19 vaccines induce immune response to Omicron*. 2022, https://www.nih.gov/news-events/nih-research-matters/covid-19-vaccines-induce-immune-response-omicron: NIH Research Matters, February 15.
14. Sofonea, M.T., et al., *From Delta to Omicron: analysing the SARS-CoV-2 epidemic in France using variant-specific screening tests (September 1 to December 18, 2021)*. 2022, https://www.medrxiv.org/content/10.1101/2021.12.31.21268583v1: MedRxiv, January 1.
15. Lloyd-Smith, J.O., et al., *Superspreading and the effect of individual variation on disease emergence.* Nature, 2005. **438**(7066): p. 355-9.
16. Brooks-Pollock, E., et al., *Impact of voluntary risk-mitigation behaviour on transmission of the Omicron SARS-CoV-2 variant in England*. 2022, https://www.medrxiv.org/content/10.1101/2022.01.26.22269540v2: medRxiv, February 16.

17. Kozlov, M., *Omicron's feeble attack on the lungs could make it less dangerous.* Nature, 2022. **601**(7892): p. 177.
18. Imbriano, G., et al., *Online Survey of the Impact of COVID-19 Risk and Cost Estimates on Worry and Health Behavior Compliance in Young Adults.* Front Public Health, 2021. **9**: p. 612725.
19. Su, Z., et al., *Mind the "worry fatigue" amid Omicron scares.* Brain Behav Immun, 2022. **101**: p. 60-61.
20. Tyson, R.C., et al., *The Timing and Nature of Behavioural Responses Affect the Course of an Epidemic.* Bull Math Biol, 2020. **82**(1): p. 14.
21. Harris, J.E., *Geospatial Analysis of a COVID-19 Outbreak at the University of Wisconsin – Madison: Potential Role of a Cluster of Local Bars.* Epidemiology & Infection, 2022. **In press**(Preprant at https://www.nber.org/papers/w28132).
22. Springborn, M., et al., *Accounting for behavioral responses during a flu epidemic using home television viewing.* BMC Infect Dis, 2015. **15**: p. 21.
23. Jewell, S., et al., *It's complicated: characterizing the time-varying relationship between cell phone mobility and COVID-19 spread in the US.* NPJ Digit Med, 2021. **4**(1): p. 152.
24. Elarde, J., et al., *Change of human mobility during COVID-19: A United States case study.* PLoS One, 2021. **16**(11): p. e0259031.
25. Google, *Community Mobility Reports*. 2022, https://www.google.com/covid19/mobility/: Accessed March 3.
26. Harris, J.E., *COVID-19 Incidence and Hospitalization During the Delta Surge Were Inversely Related to Vaccination Coverage Among the Most Populous U.S. Counties.* Health Policy Technol, 2021: p. 100583.
27. U.S. Centers for Disease Control and Prevenetion, *COVID Data Tracker: Variant Proportions*. 2022, https://covid.cdc.gov/covid-data-tracker/#variant-proportions: Accessed January 20.
28. Google, *Mobility Report CSV Documentation*. 2022, https://www.google.com/covid19/mobility/data_documentation.html?hl=en: Accessed March 3.
29. White House COVID-19 Team, *COVID-19 Community Profile Report*. 2022, https://healthdata.gov/Health/COVID-19-Community-Profile-Report/gqxm-d9w9: HealthData.gov, Excel Files for 12/7/2021 through 3/1/2022.
30. U.S. Centers for Disease Control and Prevenetion, *At A Glance: CDC/ATSDR Social Vulnerability Index*. 2021, https://www.atsdr.cdc.gov/placeandhealth/svi/at-a-glance_svi.html: Agency for Toxic Substances and Disease Registry, Updated August 39.
31. U.S. Centers for Disease Control and Prevenetion, *COVID-19 Vaccinations in the United States,County*. 2022, https://data.cdc.gov/Vaccinations/COVID-19-Vaccinations-in-the-United-States-County/8xkx-amqh: Accessed March 7.
32. Joliffe, I.T., *Principal Component Analysis, 2nd Edition*. 2002, New York: Springer.
33. StataCorp, *Stata Statistical Software: Release 17*. 2021, College Station, TX: StataCorp LLC.

34. Harris, J.E., *Estimated Fraction of Incidental COVID Hospitalizations in a Cohort of 250 High-Volume Hospitals Located in 164 Counties*. 2022, https://www.medrxiv.org/content/10.1101/2022.01.22.22269700v1: MedRxiv, January 24.
35. Hallett, T.B., et al., *Declines in HIV prevalence can be associated with changing sexual behaviour in Uganda, urban Kenya, Zimbabwe, and urban Haiti.* Sex Transm Infect, 2006. **82 Suppl 1**: p. i1-8.
36. Lau, J.T., et al., *Monitoring community responses to the SARS epidemic in Hong Kong: from day 10 to day 62.* J Epidemiol Community Health, 2003. **57**(11): p. 864-70.
37. Rubin, G.J., et al., *Public perceptions, anxiety, and behaviour change in relation to the swine flu outbreak: cross sectional telephone survey.* BMJ, 2009. **339**: p. b2651.
38. Ibuka, Y., et al., *The dynamics of risk perceptions and precautionary behavior in response to 2009 (H1N1) pandemic influenza.* BMC Infect Dis, 2010. **10**: p. 296.
39. Chen, F.H., *Rational behavioral response and the transmission of STDs.* Theor Popul Biol, 2004. **66**(4): p. 307-16.
40. Angrist, J.D., G.W. Imbens, and D.B. Rubin, *Identification of Causal Effects Using Instrumental Variables.* Journal of the American Statistical Association, 1996. **91**(434).

Appendix

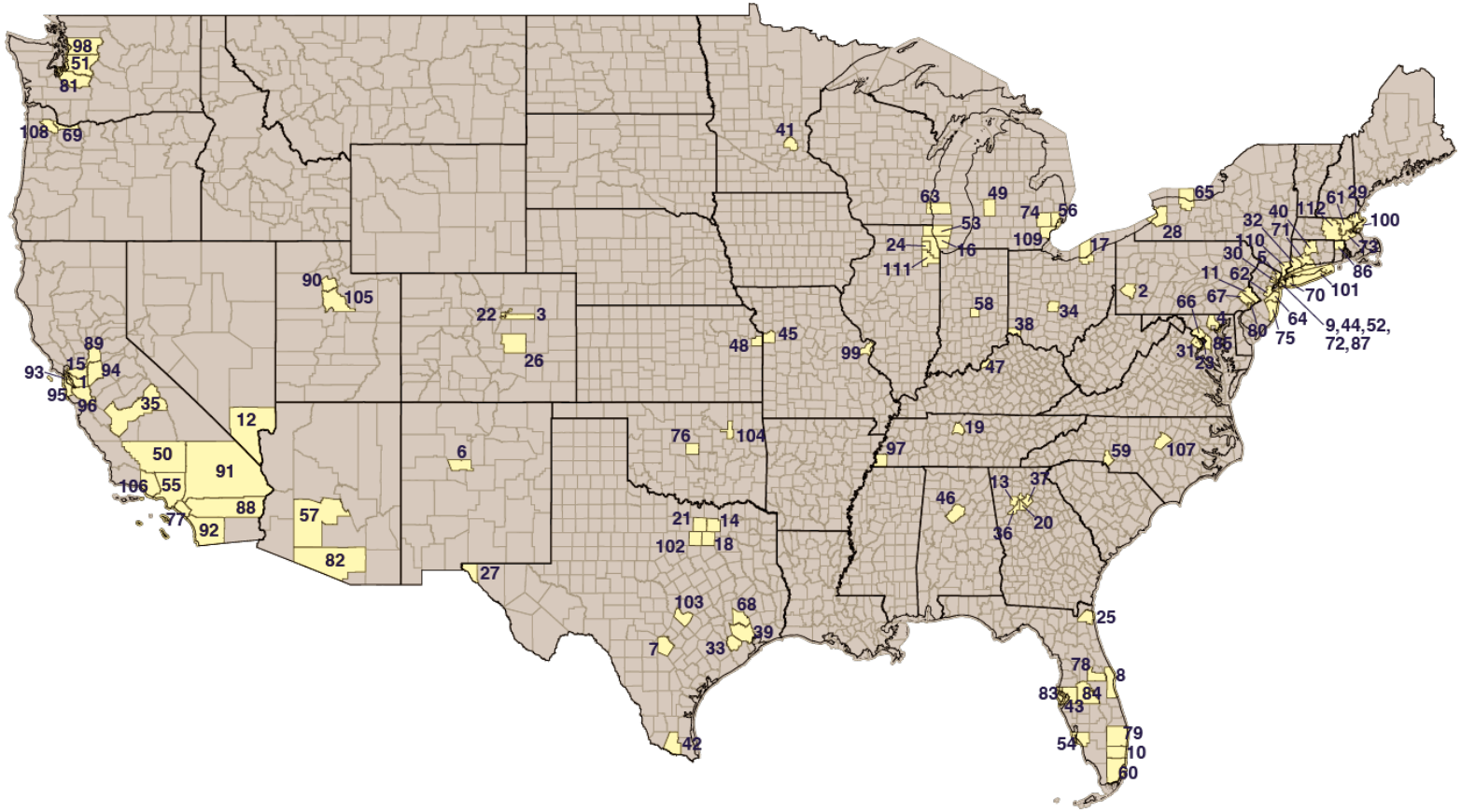

Fig. A. Initial Sample of 112 U.S. Counties with Population ≥ 600,000. All counties are numbered in accordance with the legend below. State boundaries are indicated by the thicker black lines.

Fig. A. Initial Sample of 116 Counties, with population in thousands, listed in alphabetical order.

#	County	State	Pop (000)	#	County	State	Pop (000)	#	County	State	Pop (000)	#	County	State	Pop (000)
1	Alameda	CA	1,671	29	Essex	MA	789	57	Maricopa	AZ	4,485	85	Prince George's	MD	909
2	Allegheny	PA	1,216	30	Essex	NJ	799	58	Marion	IN	965	86	Providence	RI	639
3	Arapahoe	CO	657	31	Fairfax	VA	1,148	59	Mecklenburg	NC	1,110	87	Queens	NY	2,254
4	Baltimore	MD	827	32	Fairfield	CT	943	60	Miami-Dade	FL	2,717	88	Riverside	CA	2,471
5	Bergen	NJ	932	33	Fort Bend	TX	812	61	Middlesex	MA	1,612	89	Sacramento	CA	1,552
6	Bernalillo	NM	679	34	Franklin	OH	1,317	62	Middlesex	NJ	825	90	Salt Lake	UT	1,160
7	Bexar	TX	2,004	35	Fresno	CA	999	63	Milwaukee	WI	946	91	San Bernardino	CA	2,180
8	Brevard	FL	602	36	Fulton	GA	1,064	64	Monmouth	NJ	619	92	San Diego	CA	3,338
9	Bronx	NY	1,418	37	Gwinnett	GA	936	65	Monroe	NY	742	93	San Francisco	CA	882
10	Broward	FL	1,953	38	Hamilton	OH	817	66	Montgomery	MD	1,051	94	San Joaquin	CA	762
11	Bucks	PA	628	39	Harris	TX	4,713	67	Montgomery	PA	831	95	San Mateo	CA	767
12	Clark	NV	2,267	40	Hartford	CT	892	68	Montgomery	TX	607	96	Santa Clara	CA	1,928
13	Cobb	GA	760	41	Hennepin	MN	1,266	69	Multnomah	OR	813	97	Shelby	TN	937
14	Collin	TX	1,035	42	Hidalgo	TX	869	70	Nassau	NY	1,357	98	Snohomish	WA	822
15	Contra Costa	CA	1,154	43	Hillsborough	FL	1,472	71	New Haven	CT	855	99	St. Louis	MO	994
16	Cook	IL	5,150	44	Hudson	NJ	672	72	New York	NY	1,629	100	Suffolk	MA	804
17	Cuyahoga	OH	1,235	45	Jackson	MO	703	73	Norfolk	MA	707	101	Suffolk	NY	1,477
18	Dallas	TX	2,636	46	Jefferson	AL	659	74	Oakland	MI	1,258	102	Tarrant	TX	2,103
19	Davidson	TN	694	47	Jefferson	KY	767	75	Ocean	NJ	607	103	Travis	TX	1,274
20	DeKalb	GA	759	48	Johnson*	KS	602	76	Oklahoma	OK	797	104	Tulsa	OK	652
21	Denton	TX	887	49	Kent	MI	657	77	Orange	CA	3,176	105	Utah	UT	636
22	Denver	CO	727	50	Kern	CA	900	78	Orange	FL	1,393	106	Ventura	CA	846
23	Dist. Columbia	DC	706	51	King	WA	2,253	79	Palm Beach	FL	1,497	107	Wake	NC	1,112
24	DuPage	IL	923	52	Kings	NY	2,560	80	Philadelphia	PA	1,584	108	Washington	OR	602
25	Duval	FL	958	53	Lake	IL	697	81	Pierce	WA	905	109	Wayne	MI	1,749
26	El Paso	CO	720	54	Lee	FL	771	82	Pima	AZ	1,047	110	Westchester	NY	968
27	El Paso	TX	839	55	Los Angeles	CA	10,039	83	Pinellas	FL	975	111	Will	IL	691
28	Erie	NY	919	56	Macomb	MI	874	84	Polk	FL	725	112	Worcester	MA	831

* Johnson County KS excluded from analytic sample due to missing data on the traffic component of Google Mobility Reports.

Table A displays the estimated coefficients (ζ_k, k = 1, …, 6) derived from the principal component analysis of Google mobility measures. The Residential measure has a negative coefficient, as increases in visits and duration of stay at residences reflect a decrease in mobility. Aside from the Parks mobility measure, all coefficients have approximately the same absolute values.

Table A. Estimated Coefficients and Unexplained Variances of the First Principal Component of Six Google Mobility Measures

Google Mobility Measure	*Coefficient*	*Proportion Unexplained Variance*
Retail & Recreation	0.4701	0.095
Grocery & Pharmacy	0.4188	0.282
Parks	0.2037	0.830
Transit Stations	0.4183	0.284
Workplaces	0.4223	0.270
Residential	–0.4572	0.145

Table B shows the estimates of the parameters (β_t, t = 2, …, xx) of the fixed-effects model of equation (1). Parameter β_1 for the reference category was set equal to 1.

Table B. Estimated Parameters of the Fixed-Effects Model of Equation (1)*

Parameter	*Estimate*	*95% Confidence Interval*
β_2	–0.549	–14.315, 13.247
β_3	–2.816	–16.582, 10.950
β_4	–8.810	–22.575, 4.957
β_5	–20.146	–33.913, –6.380
β_6	–9.069	–22.835, 4.607
β_7	37.663	23.896, 51.429
β_8	17.331	3.573, 31.106
β_9	19.421	5.655, 33.188
β_{10}	16.537	2.771, 30.304
β_{11}	21.235	7.469, 35.001
β_{12}	12.777	–0.989, 26.543
β_{13}	11.500	–2.266, 25.266

*Total of 1,443 observations on 111 groups (13 observations per group). R^2= 0.673. Model estimated by ordinary least squares.

Table C below shows the results of our cross-section model of equation (2). Specification A includes only the county specific change in mobility (Δx) as a covariate. Specification B adds

average household size as a covariate, while specification C includes the social vulnerability index and our two indicators of vaccination participation.

Table C. Estimated Parameters of the Cross-Sectional Model of Equation (2).*			
Explanatory Variable	*Specification A*	*Specification B*	*Specification C*
Change in Mobility Indicator (Δx)	**0.0124** (0.0032)	**0.0096** (0.0032)	**0.0090** (0.0033)
Average Household Size		**0.2830** (0.0904)	**0.2524** (0.0972)
Social Vulnerability Index			0.1643 (0.1172)
Percent Vaccine Series Complete			0.0048 (0.0030)
Booster Doses per 100 Population			–0.0007 (0.0038)
Constant Term	**2.2435** (0.0959)	**1.3836** (0.2897)	**1.0638** (0.3405)
R^2 statistic	0.1205	0.1937	0.2243

*In all specifications, the dependent variable was the logarithm of the cumulative case incidence per 100 population between the week ending January 10, 2022 (t = 6) and the week ending February 28, 2022 (t = 13) per 100 population. There was a total of 111 observations. All models estimated by population-weighted least squares. Highlighted in bold are parameter estimates significantly different from 0 (2-sided t-test, $p < 0.05$). Standard errors are shown in parentheses below each parameter estimate.